

# FEDHM: Efficient Federated Learning for Heterogeneous Models via Low-rank Factorization\*

Dezhong Yao<sup>1</sup>, Wanning Pan<sup>1</sup>, Yao Wan<sup>1</sup>, Hai Jin<sup>1</sup>, Lichao Sun<sup>2</sup>  
<sup>1</sup>Huazhong University of Science and Technology, Wuhan, China  
<sup>2</sup>Lehigh University, USA  
 {dyao, pwn, wanyao, hjin}@hust.edu.cn, lis221@lehigh.edu

## Abstract

The underlying assumption of recent federated learning (FL) paradigms is that local models usually share the same network architecture as the global model, which becomes impractical for mobile and IoT devices with different setups of hardware and infrastructure. A scalable federated learning framework should address heterogeneous clients equipped with different computation and communication capabilities. To this end, this paper proposes FEDHM, a novel federated model compression framework that distributes the heterogeneous low-rank models to clients and then aggregates them into a global full-rank model. Our solution enables the training of heterogeneous local models with varying computational complexities and aggregates a single global model. Furthermore, FEDHM not only reduces the computational complexity of the device, but also reduces the communication cost by using low-rank models. Extensive experimental results demonstrate that our proposed FEDHM outperforms the current pruning-based FL approaches in terms of test Top-1 accuracy (4.6% accuracy gain on average), with smaller model size (1.5× smaller on average) under various heterogeneous FL settings.

## 1. Introduction

Federated Learning (FL) [23, 24] is a collaborative learning framework that allows each local client to train a global model without sharing local private data. Due to its privacy-preserving property, it is widely used or deployed on mobile and IoT devices. Although there are various FL frameworks nowadays, a most general FL paradigm consists of the following steps: (1) the server sends the global model to selected clients in each communication round, (2) each selected client trains the local model with its private data, (3) the clients send their trained local models back to the server, and (4) the server aggregates the local models to update the

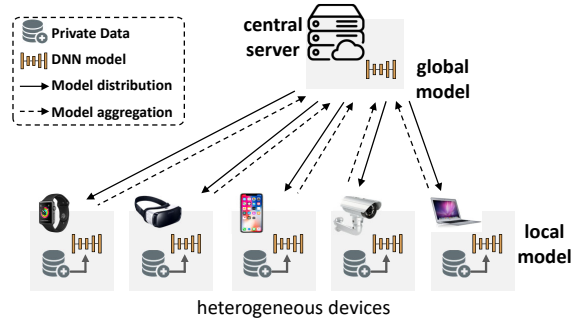


Figure 1. The FedAvg framework for heterogeneous computation scenario. The local trained models on each device share the same model architecture, which is inefficient for the resource-constrained devices.

global model and repeats the first step until the global model converges. However, the FL paradigm is still a general definition and would face many challenges in practice [9, 34]. One of the urgent challenges of FL is heterogeneity that includes both data heterogeneity and system heterogeneity.

**Data Heterogeneity.** In FL, since the data is naturally distributed among different clients, the data distribution could always be non-IID and unbalanced, which implies the local data can not represent the global data distribution [35]. **System Heterogeneity.** Clients in FL may have varying compute speeds due to hardware differences [14, 19]. As shown in Figure 1, some clients may be mobile phones, while others could be laptops equipped with GPUs. However, it is inefficient to require different clients to train the same model in such heterogeneous environments. One straightforward solution is to train heterogeneous models according to the clients’ computing speed and memory, a.k.a., *model heterogeneity*. For example, a smartwatch has resource-constrained computing resources, memory, and battery than a smartphone or laptop; thus, the smartwatch can only support a small training model in practice.

Heterogeneity presents many fundamental challenges to FL, including convergence stability, communication over-

\*Under review

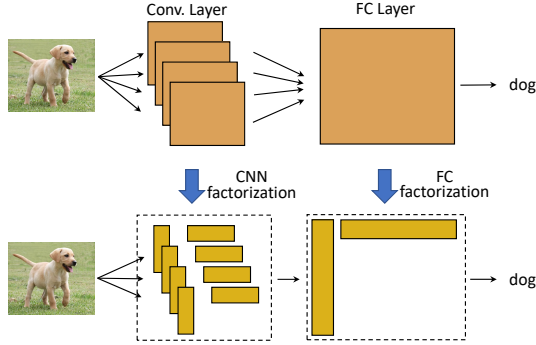


Figure 2. FC layer and CNN layer factorization. The number of parameters is significantly reduced.

heads, and model aggregation [9]. To address the data heterogeneity, the most recent work in FL have proposed modified loss functions or model aggregation mechanisms [1, 10, 17, 18, 21, 29, 33, 40]. However, very few works tackle the model heterogeneity, where different clients own different sizes of the training model due to its computing resource and memory capacity. HeteroFL [6] is the state-of-the-art method that aims to address heterogeneous clients with heterogeneous computation and communication capabilities in FL. HeteroFL applies uniform channel pruning (width slimming) for each client model and aggregates the clients’ models by channels on the server-side. However, HeteroFL suffers from two major limitations: (1) The small models obtained from naive uniform pruning can not be well-trained in FL. (2) The small model will be unfairly treated during aggregation by channels, ignoring the small models’ sparse information.

To address the shortcomings of HeteroFL, we propose a federated model compression mechanism for model heterogeneity in FL, FEDHM, which enables multiple devices to train heterogeneous local models with different computational complexities. Our key idea is to compress the large model into small models using low-rank factorization and distribute the compressed model to resource-constrained devices to achieve the local training. Specifically, FEDHM factorizes deep neural networks (DNNs) to a small and factorized form while preserving the model’s capacity. Subsequently, the server will gather the trained heterogeneous local models from the selected clients and recover each local model to a full-rank model in the same network architecture. Next, the global model can be easily aggregated from these recovered full-rank models. Note that both model factorization and model shape alignment are computed on the server, which is efficient and reduces communication costs. Overall, the contributions of this paper are as follows:

- FEDHM is the first work that utilizes the low-rank factorization mechanisms of DNNs to solve the model heterogeneity challenge in federated learning.

- Our approach outperforms the current state-of-the-art, i.e., HeteroFL, and significantly reduces the communication costs for model training.
- Our extensive experiments and analysis on various benchmark datasets and FL settings demonstrate the efficiency and effectiveness of our proposed approach.

## 2. Preliminaries

**Federated Learning.** Federated Learning aims to train a global model  $w$  from locally distributed data  $\mathcal{D} = \cup\{\mathcal{D}_p\}_{p=1}^P$  across  $P$  participant heterogeneous devices. The global model is constructed by  $L$  layers parameters  $w = \{W_1, W_2, \dots, W_L\}$ . Given a rank shrinkage ratio  $r$ , the model is factorized to a low-rank model  $w^r$ . After the low-rank model  $w_p^r$  is trained on local data  $\mathcal{D}_p$ , it will be recovered to a full-rank model and aggregate into a global model  $w_t = \frac{1}{P} \sum_{p=1}^P w_{p,t}^r$  at iteration  $t$ .

**Low-rank Factorized Training.** The forward propagation rule of a fully-connected (FC) layer can be expressed as  $\sigma(xW)$  where  $x \in \mathbb{R}^m, W \in \mathbb{R}^{m \times n}$  and  $\sigma(\cdot)$  represents arbitrary non-linear activation function. A factorized FC layer can then be represented by  $\sigma(xUV^T)$  where  $U \in \mathbb{R}^{m \times r}, V^T \in \mathbb{R}^{r \times n}$  and  $r$  is the selected rank for the low-rank factorization such that  $UV^T$  is geometrically close to  $W$ . In low-rank factorized training, only  $U$  and  $V^T$  are held in memory and trained by participating clients.

### 2.1. Motivation

System heterogeneity is a major burden for current distributed computing, especially for FL [3, 14]. The devices in federated settings may have varying computational capabilities due to hardware differences. Additionally, some devices may dedicate their resources to federated training, while others may need to share resources with background tasks. With those underlying requirements, we have to limit the model complexity for the resource-constrained devices to train on their data or exclude those devices from federated training. Both of them will degrade the performance of the global model [6]. It is a natural motivation to distribute the compressed models to the devices according to their computation capabilities.

In typical FL algorithms, such as FedAvg [24], each local model  $w_p$  shares the same network architecture with the global model  $w$ . The server receive local model and aggregate them into a global model by averaging  $w = \frac{1}{P} \sum_{p=1}^P w_p$ . Thus, it is difficult to learn the data knowledge from the resource-constrained devices by training a large local model.

This work aims to release the constraint that each local model needs to share the same network architecture as the global model. Therefore, a resource-constrained client can

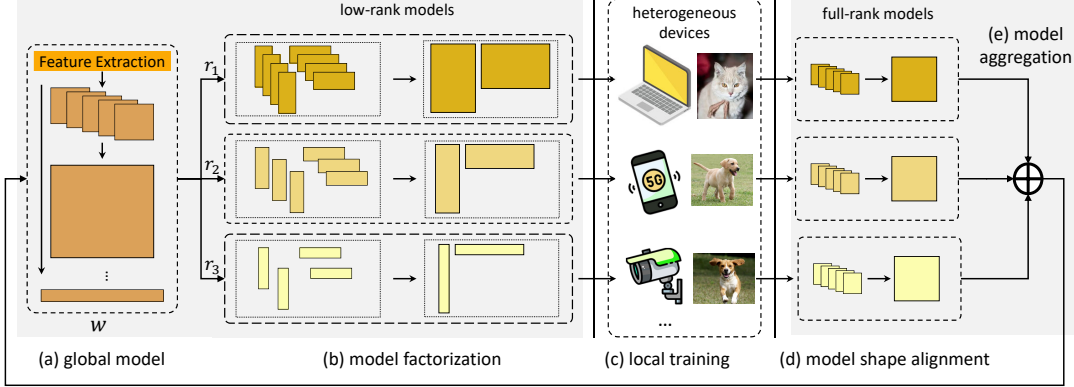


Figure 3. Overview of FEDHM. The global model  $w$  is low-rank factorized to small models and distributed to three clients. The model factorization, model recovery, and model aggregation steps (a), (b), (d), and (e) are in the server side. Only local training step (c) runs in the client side.

train a small local model and aggregate with other models in different network architecture on the server.

### 3. Federated Model Compression

#### 3.1. Overview of FEDHM

FEDHM consists of three main components, *i.e.* (1) *local factorized training*, (2) *model shape alignment*, and (3) *model aggregation*. Local factorized training allows clients with heterogeneous hardware resources to train pre-factorized low-rank models with different ranks. Then, each client can make the best utilization of its hardware resources. For instance, a cell phone client with 8G memory capacity can only afford to train a factorized low-rank ResNet-18 with rank ratio at  $\frac{1}{8}$ , but a desktop client, on the other hand, with 16G memory capacity can afford to train a full-rank ResNet-18. Upon receiving the factorized models, FEDHM conducts model shape alignment to transform the factorized low-rank models with different ranks back to full-rank shapes. The transformed models have identical shapes. For instance, central model shape alignment transforms factorized models  $U \in \mathbb{R}^{m \times r}$ ,  $V^T \in \mathbb{R}^{r \times n}$  with different  $r$ s back to  $W \in \mathbb{R}^{m \times n}$ . FEDHM finally conducts central aggregation among the transformed models using weighted coordinate-wise averaging. An overview of our federated model decomposition is illustrated in Figure 3. The global model  $w$  is factorized to different models and distributed to suitable devices.

#### 3.2. Local Factorized Training

A  $L$ -layer neural network can be denoted as:  $\{W_1, W_2, \dots, W_L\}$ . The pre-factorized low-rank version of such network can be then represented as  $\{U_1, V_1, U_2, V_2, \dots, U_L, V_L\}$ . In heterogeneous FL, each client is allowed to train a pre-factorized neural network with rank  $r$  such that its hardware resources are fully

utilized. Before the local training stage, central server factorizes the global model with different ranks and broadcasts the factorized models to the corresponding participating clients. After receiving the assigned factorized model, the clients use local private data to train it and return back to server.

**Convolution Layer Factorization.** For a 2D convolution layer, an input with dimension  $(m, H, W)$  convolved with  $n$  convolution filters of dimension  $(m, k, k)$  to create a  $n$ -channel output feature map. In our notation,  $H, W$  denote the height and width of the input feature map and  $k$  denotes the shape of a convolution filter. In order to reduce the computational and memory cost, we use the low-rank factorization to modify the architecture of the convolution layers. The core idea is to replace full rank vanilla convolution layers with factorized versions such that the model size and computation complexity are both reduced.

There are more than one way to adopt factorized convolution layer. In FEDHM, we conduct the following strategy for convolution layer factorization, which follows the strategy of [11]. For a 2D convolution layer, the parameter matrices is a 4D tensor with dimension  $(m, n, k, k)$  where  $m, n, k$  denote input channels, output channels, and size of convolution filters. Instead of factorizing the 4D tensor of a convolution layer directly, we consider factorizing the unrolled 2D matrix. Unrolling the 4D tensor  $W$  leads to a 2D matrix with shape  $(mk, nk)$ . Then factorizing  $W \in \mathbb{R}^{mk \times nk}$  leads to  $U \in \mathbb{R}^{mk \times r}$ ,  $V^T \in \mathbb{R}^{r \times nk}$  with a specific choice of  $r$ . Reshaping the factorized  $U, V$  back to 4D tensors leads to  $U \in \mathbb{R}^{m \times r \times k \times 1}$ ,  $V^T \in \mathbb{R}^{r \times n \times 1 \times k}$ . Therefore, factorizing a convolution layer with dimension  $(m, n, k, k)$  returns two convolution layers with dimensions of  $(m, r, k, 1)$  (a convolution layer with  $r$  ( $k \times 1$ ) convolution filters) and  $(r, n, 1, k)$  (a convolution layer with  $n$  ( $1 \times k$ ) convolution filters). An alternative approach to our proposed low-rank factorization is to directly conduct

---

**Algorithm 1:** FEDHM: Federated Learning for Heterogeneous Models.

---

**Input :** Dataset  $[\mathcal{D}_p]_{p=1}^P$  distributed on  $P$  clients, fraction of participants  $C$ , total communication rounds  $T$ , local epochs  $E$ , learning rate  $\eta$ , rank shrinkage ratios  $[r_i]_{i=1}^T$ , hyper-parameter  $\rho$ .

**Output:** Final model  $w_{T+1}$

**ServerExecute:** // server side

- 1 initialize  $L$ -layer network  $w_0 = \{W_1, \dots, W_L\}$
- 2 **for**  $t = 1, \dots, T$  **do**
- 3     **for**  $r = 1, \dots, \Gamma$  **do**
- 4         factorize network  $[\rho, L]$ -layers to a hybrid network  $w_t^r$
- 5         **for**  $p = 1, \dots, P$  **do in parallel**
- 6             send the model  $w_t^r$  to client  $p$  based on capability
- 7              $w_{p,t+1}^r \leftarrow \text{LocalUpdate}(w_t^r, p)$
- 8         recover network  $w_{t+1}$  using Eq. 1
- 9 **return**  $w_{T+1}$

**LocalUpdate**( $w_t^r, p$ ): // client side

- 10  $h_{p,0} \leftarrow w_t^r$
- 11 **for**  $i = 1, \dots, E$  **do**
- 12     find optimal  $h_{p,i}$  on  $\mathcal{D}_p$  with Frobenius decay
- 13 **return**  $h_{p,E}$  to server

---

tensor decomposition, *e.g.*, the CP and Tucker decomposition [15, 27] to directly factorize the 4D tensor weights. In this work, we do not consider tensor decomposition, as they have lower accuracy and more computational cost than low-rank factorization [11].

**Hybrid Network Architecture.** Since the low-rank factorized network is an approximation of the original network, where  $UV^\top$  is geometrically close to the un-factorized weight  $W$ , an approximation error will be introduced when factorizing each layer. This approximation errors in the early layers can be accumulated and propagated to the later layers, which will significantly impact on the model accuracy [32]. A straightforward idea is to only factorize the later layers to preserve the final model accuracy. Moreover, especially for CNNs, the number of parameters in later layers dominates the entire network size, *e.g.*, the last 3 bottleneck residual blocks of ResNet-50 contains up to  $\sim 60\%$  of the entire model parameters. Thus, factorizing the later layers does not sacrifice the model compression rate. To achieve this goal, we implement a hybrid network architecture to control the first  $\rho$  layers are not factorized, *i.e.*,  $\{W_1, W_2, \dots, W_\rho, U_{\rho+1}, V_{\rho+1}^\top, \dots, U_L, V_L^\top\}$ . We treat  $\rho$  as a hyper-parameter that balances the model compression ratio and the final model accuracy. Here, every model is a hybrid network architecture with the tuned values of  $\rho$ .

**Initialization and Regularization of Factorized Layers.**

As illustrated in [11], to improve the performance, the low-rank model initialized with spectral initialization(SI) should be regularized with Frobenius decay(FD). The Frobenius

Layer	# Params.	Comp. Complexity
Vanilla FC	$mn$	$\mathcal{O}(mn)$
Factorized FC	$r(m+n)$	$\mathcal{O}(r(m+n))$
Vanilla Conv.	$mnk^2$	$\mathcal{O}(mnk^2HW)$
Factorized Conv.	$rk(m+n)$	$rkHW(m+n)$
Factorized Conv. in [32]	$r(mk^2+n)$	$rHW(mk^2+n)$

Table 1. Comparison of parameters and computational complexity for full-rank and low-rank FC and Conv. layers.

decay penalty on matrices  $U, V^\top$  is  $\frac{\lambda}{2} \|UV^\top\|_F^2$  where  $\lambda$  is the coefficient of regularization which controls the strength of the penalty. Since the spectral initialization is naturally implemented on the model distribution process (by using SVD to decompose the model), we replace the weight decay with Frobenius decay for local training.

### 3.3. Model Shape Alignment and Aggregation

After the server receives the local update  $w_{p,t+1}^r$  from the  $p$ -th client, FEDHM conducts model shape alignment via transforming  $UV^\top$  back to  $\widetilde{W}$ , which shares the same shape as  $W$  for each factorized layer in the hybrid architecture. FEDHM then conducts model aggregation to a global network  $w_{p,t+1}$ . The reshaped local full-rank model is represented as  $w_{p,t+1} = \{W_1, W_2, \dots, W_\rho, \dots, \widetilde{W}_{\rho+1}, \dots, \widetilde{W}_L\}$ .

As the amount of parameters represents the knowledge of each model, we use weighted mechanism to aggregate the reshaped local models into the global model. Suppose the participants number in each round is  $P$ , the weight aggregation method is calculated as follows:

$$w_{t+1} = \frac{1}{P} \sum_p \alpha_p w_{p,t+1}, \quad \alpha_p = \frac{\exp \frac{\gamma_p}{\tau}}{\sum_p \exp \frac{\gamma_p}{\tau}}, \quad (1)$$

where  $\gamma_p = r/\text{rank}(w)$  denotes the rank ratio for the client  $p$ , and  $\tau$  denotes the softmax temperature.

### 3.4. Computational Complexity and Model Size

We summarize the computational complexity and the number of parameters in the vanilla and low-rank FC, convolution layers in Table 1. For model sizes of both FC layer, low-rank factorization reduces the model dimension from  $(m, n)$  to  $(m, r), (r, n)$ . For computation complexity of FC layer, it is also easy to see that  $xW$  requires  $\mathcal{O}(mn)$  and  $xUV^\top$  requires  $\mathcal{O}(mr + rn) = \mathcal{O}r(m+n)$ . For a convolution layer, the un-factorized layer has dimension  $(m, n, k, k)$  while the factorized low-rank layer has dimensions  $(m, r, k, 1), (r, n, 1, k)$  as discussed before. Thus, the factorized convolution reduces the total number of parameters from  $mnk^2$  to  $rmk + rnk$ . For computation complexity of convolution layers, a un-factorized convolution layer requires  $\mathcal{O}(mnk^2HW)$  as there are  $n$  filters with size  $m \times k \times k$ , and the filter has to convolve over  $H \times W$  pixels

DataSet	Setting	HeteroFL		HeteroFL-V2		HeteroFL-V3		Width Slimming (FedAvg)		FEDHM	
		Parameters	Accuracy	Parameters	Accuracy	Parameters	Accuracy	Parameters	Accuracy	Parameters	Accuracy
CIFAR-10	IID	11.17M	93.19	4.29M( $\times 2$ )	93.19	2.80M( $\times 3$ )	93.18	1.37M( $\times 4$ )	92.66	<b>11.17M</b>	<b>93.50</b>
		4.29M	93.13	2.80M	92.77	1.37M	92.14			<b>4.16M</b>	<b>93.52</b>
		2.80M	92.93	1.37M	92.01					<b>2.21M</b>	<b>93.49</b>
		1.37M	92.16							<b>1.24M</b>	<b>93.43</b>
	Non-IID	11.17M	91.57	4.29M( $\times 2$ )	91.14	2.80M( $\times 3$ )	91.05	1.37M( $\times 4$ )	90.21	<b>11.17M</b>	<b>91.59</b>
		4.29M	<b>91.53</b>	2.80M	91.03	1.37M	89.93			<b>4.16M</b>	91.51
		2.80M	91.03	1.37M	89.52					<b>2.21M</b>	<b>91.55</b>
		1.37M	90.19							<b>1.24M</b>	<b>91.47</b>
CIFAR-100	IID	21.33M	66.56	8.77M( $\times 2$ )	67.32	5.35M( $\times 3$ )	66.81	3.42M( $\times 4$ )	63.07	<b>8.40M</b>	<b>71.20</b>
		8.77M	66.39	5.35M	66.32	3.42M	65.31			<b>4.99M</b>	<b>71.24</b>
		5.35M	65.68	3.42M	65.17					<b>3.27M</b>	<b>71.31</b>
		3.42M	64.11							<b>2.71M</b>	<b>71.21</b>
	Non-IID	21.33M	67.37	8.77M( $\times 2$ )	66.76	5.35M( $\times 3$ )	67.25	3.42M( $\times 4$ )	66.69	<b>8.40M</b>	<b>67.78</b>
		8.77M	67.30	5.35M	66.04	3.42M	65.25			<b>4.99M</b>	<b>67.81</b>
		5.35M	66.26	3.42M	64.75					<b>3.27M</b>	<b>67.78</b>
		3.42M	64.56							<b>2.71M</b>	<b>67.78</b>

Table 2. Top-1 test accuracy comparison with different methods under dynamic heterogeneous setting.

(controlled by a stride size). Using the same analysis, one can easily get that the factorized low-rank convolution layer needs computation complexity of  $\mathcal{O}(mrkHW + nrkHW)$  to convolve a input with  $HW$  pixels and  $m$  input channel. We also compare our convolution layer factorization strategy against another popular factorization strategy used in Pufferfish [32] (shown in Table 1). One can see that for both model size and computation complexity, our factorization strategy balances the  $k$  term to both input dimension  $m$  and output dimension  $n$  while the strategy used by [32] push all  $k^2$  term to input dimension  $m$ . Thus, unless the input dimension is much smaller than output dimension, our strategy usually leads to smaller model size and lower computation complexity. A low-rank factorized network enjoys a smaller network of parameters and lower computational complexity which is indicated in Table 1. We notice that both the computation and communication efficiencies are improved, as the amount of communication is proportional to the number of parameters.

## 4. Experiments

In this section, we conduct experiments to answer the following questions: (1) *What is the performance of FEDHM and its baselines?* (2) *What is the efficiency of FEDHM?* (3) *What is the effectiveness of each component of FEDHM?*

### 4.1. Experiment Setup

**Datasets and Model Setting.** In the experiments, we adopt two datasets that have been widely used to evaluate FL in computer vision, i.e., CIFAR-10 and CIFAR-100 [13]. According to the complexity of datasets, we conduct experiments on CIFAR-10 and CIFAR-100 using ResNet-18 and ResNet-34, respectively. Furthermore, for the FL setting, we experiment on CIFAR-10 and CIFAR-100 for 160 and 100 communication rounds, and in each round, we sample 50% of the clients. We set the number of clients in experi-

ments to 20, and each client trains 10 epochs in every communication round.

**System Heterogeneity.** The system heterogeneity in our experiments is pre-defined as different levels of computation complexity, following [6]. To construct different computation complexity, we vary the rank ratio  $\gamma$  in  $\{0.5, 0.25, 0.125, 0.083\}$  on ResNet-18 and ResNet-34, and tune the initial low-rank layer index  $\rho$  to balance the model size and accuracy. We set the shrinkage ratio of HeteroFL in  $\{0.64, 0.50, 0.40, 0.35\}$  on ResNet-18 and ResNet-34, so as to reach a larger model size. As illustrated in [6], the computation capability of the clients may dynamically change, therefore we conduct experiments on both the dynamic and fixed scenarios. To this end, we annotate fixed heterogeneous setting for clients with a fixed assignment of computation complexity levels, and annotate the dynamic heterogeneous setting for clients uniformly sampling computation complexity levels at each communication round. We set the softmax temperature  $\tau$  to 5 and  $+\infty$  respectively, under the dynamic and fixed settings. We extend two variants based on HeteroFL (named HeteroFL-V2 and HeteroFL-V3) through changing the heterogeneous model groups to better study the impact of different model combinations. Following [6], we incorporate the static batch normalization and masking cross-entropy methods in the experiments.

**Data Heterogeneity.** Following prior works [8], we sample the disjoint Non-IID client data using the Dirichlet distribution  $\text{Dir}(\alpha)$ , where  $\alpha$  denotes the concentration parameter. Empirically, we set the  $\alpha$  to 0.5. To reduce the over-fitting on local datasets [26], we train the local models of FEDHM with self-distillation mechanism under the Non-IID setting.

**Baselines.** We compare FEDHM with the following state-of-the-art baselines in experiments.

- **FedAvg** [24] is a classic FL algorithm, which performs the aggregation using the averaging. We use it to evaluate the model performance for homogeneous settings, where each local model has the same model size.

DataSet	Setting	HeteroFL		HeteroFL-V2		HeteroFL-V3		Width Slimming(FedAvg)		FEDHM	
		Parameters	Accuracy	Parameters	Accuracy	Parameters	Accuracy	Parameters	Accuracy	Parameters	Accuracy
CIFAR-10	IID	11.17M	89.82	4.29M( $\times 2$ )	91.14	2.80M( $\times 3$ )	91.83	1.37M( $\times 4$ )	92.66	<b>11.17M</b>	<b>93.46</b>
		4.29M	89.97	2.80M	91.03	1.37M	90.15			<b>4.16M</b>	<b>93.37</b>
		2.80M	89.38	1.37M	89.52					<b>2.21M</b>	<b>93.40</b>
		1.37M	87.83							<b>1.24M</b>	<b>93.40</b>
	Non-IID	11.17M	84.49	4.29M( $\times 2$ )	87.61	2.80M( $\times 3$ )	87.46	1.37M( $\times 4$ )	90.21	<b>11.17M</b>	<b>91.22</b>
		4.29M	86.44	2.80M	86.93	1.37M	84.45			<b>4.16M</b>	<b>91.21</b>
		2.80M	86.28	1.37M	84.20					<b>2.21M</b>	<b>91.23</b>
		1.37M	84.08							<b>1.24M</b>	<b>91.17</b>
CIFAR-100	IID	21.33M	56.01	8.77M( $\times 2$ )	62.05	5.35M( $\times 3$ )	64.24	3.42M( $\times 4$ )	63.07	<b>8.40M</b>	<b>71.76</b>
		8.77M	59.23	5.35M	61.83	3.42M	61.52			<b>4.99M</b>	<b>71.79</b>
		5.35M	59.93	3.42M	59.20					<b>3.27M</b>	<b>71.81</b>
		3.42M	57.95							<b>2.71M</b>	<b>71.79</b>
	Non-IID	21.33M	53.55	8.77M( $\times 2$ )	60.42	5.35M( $\times 3$ )	64.37	3.42M( $\times 4$ )	66.69	<b>8.40M</b>	<b>67.27</b>
		8.77M	58.40	5.35M	59.16	3.42M	60.06			<b>4.99M</b>	<b>67.27</b>
		5.35M	58.61	3.42M	57.67					<b>3.27M</b>	<b>67.27</b>
		3.42M	57.20							<b>2.71M</b>	<b>67.32</b>

Table 3. Comparison with HeteroFL under fixed heterogeneous setting.

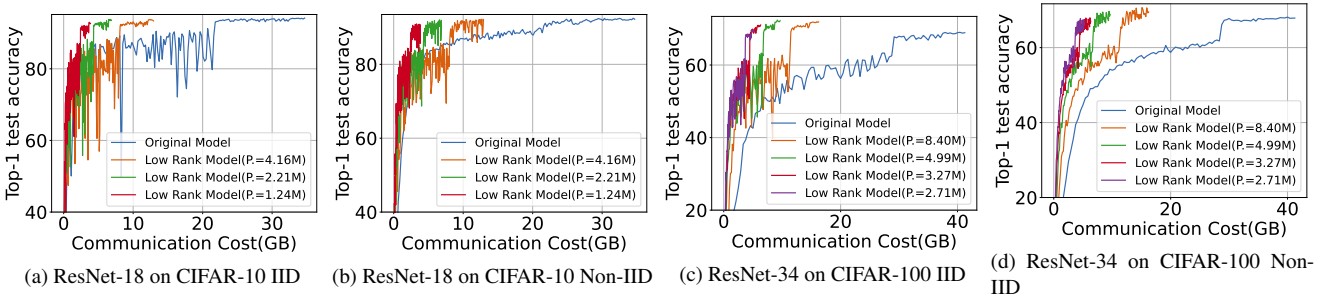


Figure 4. The test Top-1 accuracy v.s. communication cost under homogeneous setting (the participant number is 10).

- **HeteroFL** [6] leverages the network slimming strategy to compress the heterogeneous client models and aggregate them by channels.

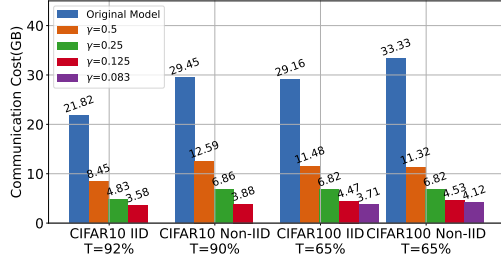
## 4.2. Performance Evaluation (RQ1)

We evaluate the Top-1 accuracy on both IID and Non-IID settings under dynamic heterogeneous FL setting. Following [6], we first evaluate the performance of the server model (the one with the largest model size) under dynamic heterogeneous setting. Furthermore, since the smaller model should be deployed on resource-constrained devices, we evaluate the performance of client models with different levels of computation complexity. In addition, we evaluate the performance of the server model and client models under fixed heterogeneous setting.

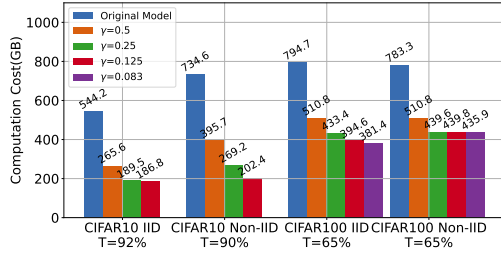
**Performance of Server and Client Models.** Table 2 shows the performance of FEDHM and baselines in terms of Top-1 test accuracy under the dynamic heterogeneous setting. From this table, it is clear to see that both the server and client models of FEDHM consistently outperforms that of baselines. When comparing with FedAvg, we can find that both the FEDHM and HeteroFL can improve the performance of the server model. Additionally, on CIFAR-100, FEDHM defeats HeteroFL in terms of Top-1 test accuracy with only half parameters of that. When comparing

FEDHM with different variants of HeteroFL, we can observe that FEDHM shows superiority in terms of the accuracy of smallest model. On CIFAR-10, FEDHM surpasses baselines by 0.77% and 1.26% in terms of Top-1 accuracy, under IID and Non-IID settings. On CIFAR-100 dataset, FEDHM surpasses HeteroFL by 5.90% and 1.09% in terms of Top-1 accuracy, under IID and Non-IID settings. The improvements for small models are helpful since the resource-constrained devices may not be able to deploy the large server model. Furthermore, we can also find that the performance gain achieved by FEDHM from low-rank factorization (compared with HeteroFL) becomes larger when switching the dataset from CIFAR-10 to CIFAR-100. We attribute it to the direct width slimming for the last convolution and classifier in HeteroFL, while in FEDHM the dimension of those is maintained. Additionally, this table also shows that the HeteroFL in Non-IID setting performs better than that in IID setting, which can be ascribed to the masking cross-entropy and weighted aggregation for classifier under the Non-IID setting.

**Performance under Fixed Heterogeneous Setting.** We conduct the same experiments in the fixed heterogeneous setting. As shown in Table 3, the performance of HeteroFL drops under fixed heterogeneous setting, while FEDHM shows the robustness. Compare the perfor-



(a) Communication cost in FL training (participants number is 10).



(b) Computation cost of each client.

Figure 5. Evaluating different compression ratio in homogeneous setting, in terms of the communication cost and computation cost to reach target Top-1 test accuracy.  $T$  denotes the specified target accuracy.

mance of the server model, FEDHM outperforms HeteroFL 1.63%/3.76% and 7.52%/2.90% in terms of test Top-1 accuracy on CIFAR10 IID/Non-IID, CIFAR100 IID/Non-IID settings. We attribute the performance drop to that HeteroFL ignores the sparse information of the small models during aggregation, and the large models face the risk of over-fitting on local data. FEDHM is not effected by the computation scenarios since FEDHM reduces over-fitting by aggregating the sparse information of the small models.

### 4.3. Efficiency Analysis (RQ2)

**Communication and Computation Cost.** We compare the factorized low-rank models and the original model before factorization, in terms of communication cost and computation cost. Figure 4 shows the test Top-1 accuracy *w.r.t.* communication cost under homogeneous setting. From this figure, we can find that low-rank models require much lower communication cost and achieve comparable Top-1 test accuracy, compared to original model. Figure 5a shows the communication cost to reach target accuracy, compared to the original model. Furthermore, FEDHM saves the communication cost  $6.1\times/7.6\times$  and  $7.9\times/8.1\times$ , under the CIFAR10 IID/Non-IID and CIFAR100 IID/Non-IID settings. Figure 5b shows that to reach target accuracy, original model requires  $2.9\times/3.6\times$  and  $2.1\times/1.8\times$  computation cost than FEDHM, under CIFAR10 IID/Non-IID and CIFAR100 IID/Non-IID settings. The experimental results confirm the effectiveness of the compression method, the method further improves the performance of client models under heterogeneous setting.

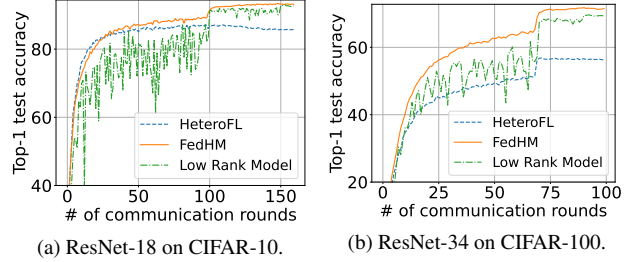


Figure 6. Evaluating different methods in terms of convergence speed of the smallest model, FEDHM and HeteroFL are evaluated under IID fixed heterogeneous setting, low-rank model is evaluated under homogeneous setting.

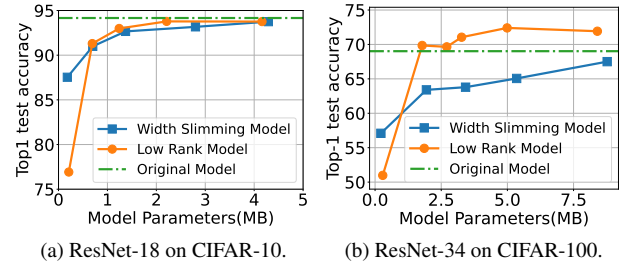


Figure 7. Comparison with width slimming model in terms of test Top-1 accuracy, evaluated under IID homogeneous setting.

**Convergence Speed under Heterogeneous Setting.** We also compare the convergence speed of FEDHM with HeteroFL under fix heterogeneous setting, as well as the smallest low-rank model(parameters of low-rank model is 1.24M and 2.71M on CIFAR-10 and CIFAR-100) under homogeneous setting, in terms of convergence speed. Figure 6 shows that FEDHM and low rank model significantly outperforms HeteroFL with fewer parameters on CIFAR-10 and CIFAR-100. From this figure, we can also find that though training the low-rank model homogeneously is able to achieve comparable performance, training with larger models in FEDHM will speed up the convergence. Overall, FEDHM consistently outperforms low-rank model in the training process, and shows more smooth learning curve compared with training low-rank model homogeneously.

### 4.4. Ablation Study (RQ3)

**Effect of Compression.** To study the effect of different compression methods, we conduct experiments on training low-rank models and width slimming models in homogeneous setting respectively. For the low-rank model with the smallest size, we remove the hybrid network structure and directly decompose all the convolution layers. As shown in Figure 7, if not compressed severely(parameters ratio  $\geq 5\%$ ), low-rank models consistently outperform width slimming model with fewer parameters. However, when removing the hybrid network structure and setting the model size as 2% (the rank of each convolution layer is  $k$ ), the performance of vanilla low-rank model will drop signifi-

Setting	FEDHM		FEDHM-V2		FEDHM-V3		Low Rank Model	
	Parameters	Accuracy	Parameters	Accuracy	Parameters	Accuracy	Parameters	Accuracy
IID	11.17M	<b>93.50</b>	4.16M( $\times 2$ )	93.33	2.21M( $\times 3$ )	93.27	1.24M( $\times 4$ )	92.99
	4.16M	<b>93.52</b>	2.21M	93.36	1.24M	93.19		
	2.21M	<b>93.49</b>	1.24M	93.35				
	1.24M	<b>93.43</b>						
Non-IID	11.17M	<b>91.59</b>	4.16M( $\times 2$ )	91.18	2.21M( $\times 3$ )	90.93	1.24M( $\times 4$ )	90.95
	4.16M	<b>91.51</b>	2.21M	91.17	1.24M	90.95		
	2.21M	<b>91.55</b>	1.24M	91.25				
	1.24M	<b>91.47</b>						

Table 4. Evaluating the effectiveness with different factorized model combination on CIFAR-10, under fixed heterogeneous setting.

cantly, i.e., from over 90% to below 80% on CIFAR-10, and from 70% to below 55% on CIFAR-100, indicating the effectiveness of hybrid network structure. From Figure 7b, we can also find that low-rank models achieve comparable performance on CIFAR-10, and better performance on CIFAR-100, when compared with the original model. This is because that SI and FD can improve the performance of low-rank models, and the model compression can lead to regularization effects.

**Aggregation of Different Models.** We conduct experiments on different low-rank models combination and extend two variants based on FEDHM (named FEDHM-V2 and FEDHM-V3), under fixed heterogeneous setting, to study the effect of aggregation. As shown in Table 4, FEDHM is robust to different models aggregation, and the performance of small model increases as aggregating with larger models. The experiment results show that the aggregation method in FEDHM will not hurt the performance of small model under fixed heterogeneous setting.

#### 4.5. Limitations of FEDHM

One limitation of FEDHM is that it introduces two extra hyper-parameters, i.e., the pre-defined rank shrinkage ratios  $[r_i]_{i=1}^L$  and initial low-rank layer  $\rho$ . As the performance of FEDHM crashes down when we decompose all the layers as shown in Figure 7, it is important to find the optimal  $\rho$  for the hybrid network. We will further implement an adaptive version to find the optimal  $\rho$  based on different clients' capabilities.

### 5. Related Work

**Federated Learning.** Federated learning (FL) distributes machine learning model to the resource-constrained edges from which data originate, emerged as a promising alternative machine learning paradigm [23,25,33,34]. FL enables a multitude of participants to construct a joint model without sharing their private training data [4,22,23,25]. Some recent work focus on compressing the parameters or transmitting partial network for efficient transmission [2,20,28,30]. However, they do not reduce the computation overhead on edge. Another line of work aims to offload partial network to the server [7,36] to tackle the computational overhead challenge, while sharing local data information may leak

privacy. Our work reduces both the communication cost and training overhead for clients.

**Heterogeneous Networks Training.** Yu et al. [39] initially present the approach to training the neural network with different widths, and US-Net [38] proposes switchable-BatchNorm to solve the statistics problem in Batch Normalization. Once-for-all [5] develops progressive pruning to train the supernet in NAS. DS-Net [16] proposes to adjust the network according to the input dynamically. The above methods are applicable in model inference. FedMD and FedDF [17,21] break the knowledge barriers among heterogeneous client models by distillation on proxy data. However, the proxy data requires additional effort to design and is not always available. HeteroFL [6] introduces the techniques in [38] into heterogeneous FL and proposes to train networks with different widths in different clients.

**Low-rank Factorization.** Low-rank factorization is a classical compression method, while it is impractical to factorize the model after training [15,31,37] in FL. Furthermore, directly training the low-rank model from scratch [12] results in the performance drop. FedDLR [28] factorizes the server model and recovers the low-rank model on the clients, reducing the communication cost while increasing the local computation cost. Pufferfish [32] improves the performance of the low-rank model by training a hybrid network and warm-up. Khodak et al. [11] study the gradient descent on factorized layers and propose improving the low-rank models' performance by SI and FD. In this paper, we utilize the low-rank factorization to handle the model heterogeneity in federated learning.

### 6. Conclusion

In this paper, we have proposed a novel heterogeneous FL framework FEDHM, reducing the communication cost and training overhead for the devices. By incorporating the low-rank decomposition approaches, FEDHM improves the performance of the server model and client models under various heterogeneous settings. The efficiency of our method can be further improved by combining other efficient FL optimizers. Comprehensive experiments and analyses verify the effectiveness of our proposed approach when compared with the state-of-the-art baselines.



## References

- [1] Durmus Alp Emre Acar, Yue Zhao, Ramon Matas Navarro, Matthew Mattina, Paul N Whatmough, and Venkatesh Saligrama. Federated learning based on dynamic regularization. *arXiv preprint arXiv:2111.04263*, 2021. 2
- [2] Alyazeed Albasyoni, Mher Safaryan, Laurent Condat, and Peter Richtárik. Optimal gradient compression for distributed and federated learning. *arXiv preprint arXiv:2010.03246*, 2020. 8
- [3] Tal Ben-Nun and Torsten Hoefler. Demystifying parallel and distributed deep learning: An in-depth concurrency analysis. *ACM Computing Surveys (CSUR)*, 52(4):1–43, 2019. 2
- [4] Keith Bonawitz, Vladimir Ivanov, Ben Kreuter, Antonio Marcedone, H Brendan McMahan, Sarvar Patel, Daniel Ramage, Aaron Segal, and Karn Seth. Practical secure aggregation for privacy-preserving machine learning. In *Proceedings of the 2017 ACM SIGSAC Conference on Computer and Communications Security*, pages 1175–1191, 2017. 8
- [5] Han Cai, Chuang Gan, Tianzhe Wang, Zhekai Zhang, and Song Han. Once-for-all: Train one network and specialize it for efficient deployment. In *International Conference on Learning Representations*, 2019. 8
- [6] Enmao Diao, Jie Ding, and Vahid Tarokh. Heterofl: Computation and communication efficient federated learning for heterogeneous clients. In *International Conference on Learning Representations*, 2020. 2, 5, 6, 8
- [7] Chaoyang He, Murali Annavam, and Salman Avestimehr. Group knowledge transfer: Federated learning of large cnns at the edge. *Advances in Neural Information Processing Systems*, 33, 2020. 8
- [8] Tzu-Ming Harry Hsu, Hang Qi, and Matthew Brown. Measuring the effects of non-identical data distribution for federated visual classification. *arXiv preprint arXiv:1909.06335*, 2019. 5
- [9] Peter Kairouz, H Brendan McMahan, Brendan Avent, Aurélien Bellet, Mehdi Bennis, Arjun Nitin Bhagoji, Kallista Bonawitz, Zachary Charles, Graham Cormode, Rachel Cummings, et al. Advances and open problems in federated learning. *arXiv preprint arXiv:1912.04977*, 2019. 1, 2
- [10] Sai Praneeth Karimireddy, Satyen Kale, Mehryar Mohri, Sashank Reddi, Sebastian Stich, and Ananda Theertha Suresh. Scaffold: Stochastic controlled averaging for federated learning. In *International Conference on Machine Learning*, pages 5132–5143. PMLR, 2020. 2
- [11] Mikhail Khodak, Neil A Tenenholtz, Lester Mackey, and Nicolo Fusi. Initialization and regularization of factorized neural layers. In *International Conference on Learning Representations*, 2020. 3, 4, 8
- [12] Jakub Konečný, H Brendan McMahan, Felix X Yu, Peter Richtárik, Ananda Theertha Suresh, and Dave Bacon. Federated learning: Strategies for improving communication efficiency. *arXiv preprint arXiv:1610.05492*, 2016. 8
- [13] A Krizhevsky. Learning multiple layers of features from tiny images. *Master’s thesis, Department of Computer Science, University of Toronto*, 2009. 5, 11
- [14] Fan Lai, Xiangfeng Zhu, Harsha V Madhyastha, and Mosharaf Chowdhury. Oort: Efficient federated learning via guided participant selection. In *15th {USENIX} Symposium on Operating Systems Design and Implementation ({OSDI} 21)*, pages 19–35, 2021. 1, 2
- [15] Vadim Lebedev, Yaroslav Ganin, Maksim Rakhuba, Ivan V Oseledets, and Victor S Lempitsky. Speeding-up convolutional neural networks using fine-tuned cp-decomposition. In *ICLR (Poster)*, 2015. 4, 8
- [16] Changlin Li, Guangrun Wang, Bing Wang, Xiaodan Liang, Zhihui Li, and Xiaojun Chang. Dynamic slimmable network. In *Proceedings of the IEEE/CVF Conference on Computer Vision and Pattern Recognition*, pages 8607–8617, 2021. 8
- [17] Daliang Li and Junpu Wang. Fedmd: Heterogenous federated learning via model distillation. *arXiv e-prints*, pages arXiv–1910, 2019. 2, 8
- [18] Qinbin Li, Bingsheng He, and Dawn Song. Model-contrastive federated learning. In *Proceedings of the IEEE/CVF Conference on Computer Vision and Pattern Recognition*, pages 10713–10722, 2021. 2
- [19] Tian Li, Anit Kumar Sahu, Ameet Talwalkar, and Virginia Smith. Federated learning: Challenges, methods, and future directions. *IEEE Signal Processing Magazine*, 37(3):50–60, 2020. 1
- [20] Paul Pu Liang, Terrance Liu, Liu Ziyin, Nicholas B Allen, Randy P Auerbach, David Brent, Ruslan Salakhutdinov, and Louis-Philippe Morency. Think locally, act globally: Federated learning with local and global representations. *arXiv preprint arXiv:2001.01523*, 2020. 8
- [21] Tao Lin, Lingjing Kong, Sebastian U Stich, and Martin Jaggi. Ensemble distillation for robust model fusion in federated learning. In *NeurIPS*, 2020. 2, 8
- [22] Quande Liu, Cheng Chen, Jing Qin, Qi Dou, and Pheng-Ann Heng. Feddg: Federated domain generalization on medical image segmentation via episodic learning in continuous frequency space. In *Proceedings of the IEEE/CVF Conference on Computer Vision and Pattern Recognition*, pages 1013–1023, 2021. 8
- [23] Brendan McMahan, Eider Moore, Daniel Ramage, Seth Hampson, and Blaise Agüera y Arcas. Communication-efficient learning of deep networks from decentralized data. In *Artificial Intelligence and Statistics*, pages 1273–1282. PMLR, 2017. 1, 8
- [24] Brendan McMahan, Eider Moore, Daniel Ramage, Seth Hampson, and Blaise Agüera y Arcas. Communication-efficient learning of deep networks from decentralized data. In *Artificial Intelligence and Statistics*, pages 1273–1282, 2017. 1, 2, 5
- [25] H Brendan McMahan, Eider Moore, Daniel Ramage, and Blaise Agüera y Arcas. Federated learning of deep networks using model averaging. *CoRR, arXiv:1602.05629*, 2016. 8
- [26] Hossein Mobahi, Mehrdad Farajtabar, and Peter Bartlett. Self-distillation amplifies regularization in hilbert space. In *Advances in Neural Information Processing Systems*, 2020. 5
- [27] Anh-Huy Phan, Konstantin Sobolev, Konstantin Sozykin, Dmitry Ermilov, Julia Gusak, Petr Tichavský, Valeriy Glukhov, Ivan Oseledets, and Andrzej Cichocki. Stable low-rank tensor decomposition for compression of convolutional

- neural network. In *European Conference on Computer Vision*, pages 522–539. Springer, 2020. 4
- [28] Zhefeng Qiao, Xianghao Yu, Jun Zhang, and Khaled B Letaief. Communication-efficient federated learning with dual-side low-rank compression. *arXiv preprint arXiv:2104.12416*, 2021. 8
- [29] Sashank Reddi, Zachary Charles, Manzil Zaheer, Zachary Garrett, Keith Rush, Jakub Konečný, Sanjiv Kumar, and H Brendan McMahan. Adaptive federated optimization. *arXiv preprint arXiv:2003.00295*, 2020. 2
- [30] Daniel Rothchild, Ashwinee Panda, Enayat Ullah, Nikita Ivkin, Ion Stoica, Vladimir Braverman, Joseph Gonzalez, and Raman Arora. Fetchsgd: Communication-efficient federated learning with sketching. In *International Conference on Machine Learning*, pages 8253–8265. PMLR, 2020. 8, 12
- [31] Tara N Sainath, Brian Kingsbury, Vikas Sindhwani, Ebru Arisoy, and Bhuvana Ramabhadran. Low-rank matrix factorization for deep neural network training with high-dimensional output targets. In *2013 IEEE international conference on acoustics, speech and signal processing*, pages 6655–6659. IEEE, 2013. 8
- [32] Hongyi Wang, Saurabh Agarwal, and Dimitris Papailiopoulos. Pufferfish: Communication-efficient models at no extra cost. *Proceedings of Machine Learning and Systems*, 3, 2021. 4, 5, 8
- [33] Hongyi Wang, Mikhail Yurochkin, Yuekai Sun, Dimitris Papailiopoulos, and Yasaman Khazaeni. Federated learning with matched averaging. In *International Conference on Learning Representations*, 2020. 2, 8
- [34] Jianyu Wang, Zachary Charles, Zheng Xu, Gauri Joshi, H Brendan McMahan, Maruan Al-Shedivat, Galen Andrew, Salman Avestimehr, Katharine Daly, Deepesh Data, et al. A field guide to federated optimization. *arXiv preprint arXiv:2107.06917*, 2021. 1, 8
- [35] Jianyu Wang, Qinghua Liu, Hao Liang, Gauri Joshi, and H Vincent Poor. Tackling the objective inconsistency problem in heterogeneous federated optimization. *arXiv preprint arXiv:2007.07481*, 2020. 1
- [36] Di Wu, Rehmat Ullah, Paul Harvey, Peter Kilpatrick, Ivor Spence, and Blesson Varghese. Fedadapt: Adaptive offloading for iot devices in federated learning. *arXiv preprint arXiv:2107.04271*, 2021. 8
- [37] Jian Xue, Jinyu Li, and Yifan Gong. Restructuring of deep neural network acoustic models with singular value decomposition. In *Interspeech*, pages 2365–2369, 2013. 8
- [38] Jiahui Yu and Thomas S Huang. Universally slimmable networks and improved training techniques. In *Proceedings of the IEEE/CVF International Conference on Computer Vision*, page 1803–1811, 2019. 8
- [39] Jiahui Yu, Linjie Yang, Ning Xu, Jianchao Yang, and Thomas Huang. Slimmable neural networks. In *International Conference on Learning Representations*, 2018. 8
- [40] Zhuangdi Zhu, Junyuan Hong, and Jiayu Zhou. Data-free knowledge distillation for heterogeneous federated learning. *arXiv preprint arXiv:2105.10056*, 2021. 2

# Supplementary Material

Paper ID: 7556

## A. Detailed Experimental Setup

In this section, we elaborate the details of experiments, including datasets and hyper-parameters. Our implementation is based on PyTorch and we use the MPI as the communication backend. All the experiments are deployed on a 256GB server with 4×Tesla V100 GPUs in parallel.

### A.1. Datasets

**CIFAR-10** CIFAR-10 [13] is the popular classification benchmark dataset, which consists of 60,000 images with the resolution of  $32 \times 32$ , covering 10 classes, with 6,000 images per class.

**CIFAR-100** Similar to CIFAR-10, CIFAR-100 [13] is a image dataset of 100 classes, with 600 images per class.

**Tiny-ImageNet** Tiny-ImageNet<sup>1</sup> contains 100,000 images of 200 classes (500 for each class) downsized to  $64 \times 64$  colored images. Each class has 500 training images, 50 validation images and 50 test images.

### A.2. Hyper-parameters in experiments

Table 5 presents the detailed experimental settings in our experiments. Note that we use MultiStepLR as scheduler, and the decay rate is set to 0.1.

Dataset	CIFAR-10	CIFAR-100	Tiny-ImageNet
Clients		20	
#Samples/client	2,500	2,500	5,000
Client Sampling Rate		0.5	
Local Epoch		10	
Batch Size		64	
Optimizer		SGD	
Momentum		0.9	
Weight decay		$1e-4$	
Learning Rate		0.1	
Model	ResNet-18	ResNet-34	ResNet-34
Communication Round	160	100	60
Milestone Round	[100, 150]	[70, 90]	[40, 55]

Table 5. Detailed experimental settings in our experiments.

## B. Hybrid Network Structure

For CIFAR-10, CIFAR-100, and Tiny-ImageNet datasets, we modify the ResNet architecture used on ImageNet, and the modified network structures are shown in Tables 6 and 7. To measure the model size and computation complexity, we also analyze the number of parameters and the number of multiply-accumulate operations (MACs) of both ResNet-18 and ResNet-34 on different datasets, as shown in Figure 8. We find that the later layers (Layer3

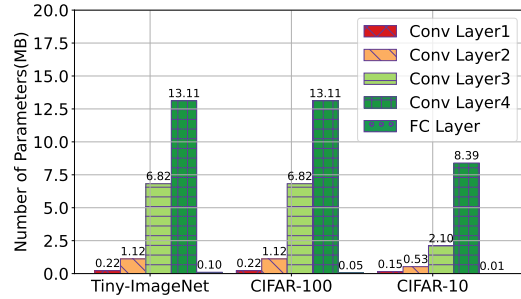
<sup>1</sup><https://www.kaggle.com/c/tiny-imagenet>

Layer Name	ResNet-18	Low Rank ResNet-18
conv1	$3 \times 3, 64, \text{stride } 1, \text{padding } 1$	$3 \times 3, 64, \text{stride } 1, \text{padding } 1$
layer1	$\begin{bmatrix} 3 \times 3, 64 \\ 3 \times 3, 64 \end{bmatrix} \times 2$	$\begin{bmatrix} 3 \times 3, 64 \\ 3 \times 3, 64 \end{bmatrix}, \begin{bmatrix} \text{conv}_u(64, 64 * \gamma, 3, 1) \\ \text{conv}_v(64 * \gamma, 64, 1, 3) \end{bmatrix} \times 2$
layer2	$\begin{bmatrix} 3 \times 3, 128 \\ 3 \times 3, 128 \end{bmatrix} \times 2$	$\begin{bmatrix} \text{conv}_u(128, 128 * \gamma, 3, 1) \\ \text{conv}_v(128 * \gamma, 128, 1, 3) \end{bmatrix} \times 4$
layer3	$\begin{bmatrix} 3 \times 3, 256 \\ 3 \times 3, 256 \end{bmatrix} \times 2$	$\begin{bmatrix} \text{conv}_u(256, 256 * \gamma, 3, 1) \\ \text{conv}_v(256 * \gamma, 256, 1, 3) \end{bmatrix} \times 4$
layer4	$\begin{bmatrix} 3 \times 3, 512 \\ 3 \times 3, 512 \end{bmatrix} \times 2$	$\begin{bmatrix} \text{conv}_u(512, 512 * \gamma, 3, 1) \\ \text{conv}_v(512 * \gamma, 512, 1, 3) \end{bmatrix} \times 4$

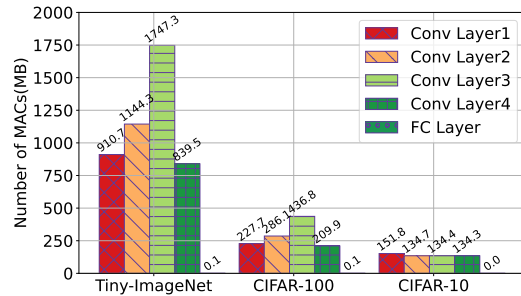
Table 6. The hybrid ResNet-18 architecture for CIFAR-10 dataset in the experiments.

Layer Name	ResNet-34	Low Rank ResNet-34
conv1	$3 \times 3, 64, \text{stride } 1, \text{padding } 1$	$3 \times 3, 64, \text{stride } 1, \text{padding } 1$
layer1	$\begin{bmatrix} 3 \times 3, 64 \\ 3 \times 3, 64 \end{bmatrix} \times 3$	$\begin{bmatrix} 3 \times 3, 64 \\ 3 \times 3, 64 \end{bmatrix} \times 3$
layer2	$\begin{bmatrix} 3 \times 3, 128 \\ 3 \times 3, 128 \end{bmatrix} \times 4$	$\begin{bmatrix} 3 \times 3, 128 \\ 3 \times 3, 128 \end{bmatrix} \times 4$
layer3	$\begin{bmatrix} 3 \times 3, 256 \\ 3 \times 3, 256 \end{bmatrix} \times 6$	$\begin{bmatrix} \text{conv}_u(256, 256 * \gamma, 3, 1) \\ \text{conv}_v(256 * \gamma, 256, 1, 3) \end{bmatrix} \times 12$
layer4	$\begin{bmatrix} 3 \times 3, 512 \\ 3 \times 3, 512 \end{bmatrix} \times 3$	$\begin{bmatrix} \text{conv}_u(512, 512 * \gamma, 3, 1) \\ \text{conv}_v(512 * \gamma, 512, 1, 3) \end{bmatrix} \times 6$

Table 7. The hybrid ResNet-34 architecture for CIFAR-100 and Tiny-ImageNet datasets in the experiments.



(a) Parameters of different layers on different datasets.



(b) MACs of different layers on different datasets.

Figure 8. Parameters and MACs of different layers of ResNet on various datasets. FC Layer denotes Fully-Connected Layer.

and Layer4) contribute the most parameters, *i.e.*, over 93% for ResNet-34 and ResNet-18, the two later layers also contribute 55.6% computation overhead on ResNet-34. From Figure 8, we can conclude that compressing the later layers can significantly reduce the communication cost and computation overhead.

DataSet	Setting	Low Rank Model			Width Slimming Model		
		Parameters	Accuracy	MACs	Parameters	Accuracy	MACs
CIFAR-10	IID	11.17M	94.16	557.22M	11.17M	94.16	557.22M
		<b>4.16M</b>	<b>93.76</b>	261.52M	4.29M	93.75	229.50M
		<b>2.21M</b>	<b>93.78</b>	173.44M	2.80M	93.17	140.20M
		<b>1.24M</b>	<b>92.99</b>	129.40M	1.37M	92.66	68.61M
	Non-IID	11.17M	92.50	11.17M	557.22M	92.50	557.22M
		<b>4.16M</b>	<b>92.25</b>	261.52M	4.29M	92.08	229.50M
		<b>2.21M</b>	<b>92.05</b>	173.44M	2.80M	91.25	140.20M
		<b>1.24M</b>	<b>90.95</b>	129.40M	1.37M	90.21	68.61M
CIFAR-100	IID	<b>8.40M</b>	<b>71.92</b>	747.24M	21.33M	69.02	1162.47M
		<b>4.99M</b>	<b>72.40</b>	633.99M	8.77M	67.50	478.19M
		<b>3.27M</b>	<b>71.05</b>	577.37M	5.35M	65.06	291.83M
		<b>2.71M</b>	<b>69.65</b>	557.90M	3.42M	63.07	187.53M
	Non-IID	<b>8.40M</b>	<b>70.69</b>	747.24M	21.33M	68.13	1162.47M
		<b>4.99M</b>	<b>69.70</b>	633.99M	8.77M	68.32	478.19M
		<b>3.27M</b>	<b>67.96</b>	577.37M	5.35M	66.73	291.83M
		<b>2.71M</b>	<b>67.74</b>	557.90M	3.42M	66.69	187.53M
Tiny-ImageNet	IID	21.38M	56.20	4649.78M	21.38M	56.20	4649.78M
		<b>8.45M</b>	<b>58.68</b>	2988.84M	8.80M	53.19	1912.71M
		<b>5.04M</b>	<b>57.27</b>	2535.85M	5.38M	52.26	1167.26M
		<b>3.33M</b>	<b>55.92</b>	2309.36M	3.44M	50.89	750.08M
	Non-IID	21.38M	56.00	4649.78M	21.38M	56.00	4649.78M
		<b>8.45M</b>	<b>55.29</b>	2988.84M	8.80M	53.61	1912.71M
		<b>5.04M</b>	<b>53.07</b>	2535.85M	5.38M	52.80	1167.26M
		<b>3.33M</b>	<b>50.37</b>	2309.36M	3.44M	50.19	750.08M

Table 8. Evaluating different methods in terms of test Top-1 accuracy under homogeneous settings.

System Setting	Data Setting	HeteroFL		HeteroFL-V2		HeteroFL-V3		Width Slimming (FedAvg)		FEDHM	
		Parameters	Accuracy	Parameters	Accuracy	Parameters	Accuracy	Parameters	Accuracy	Parameters	Accuracy
Dynamic	IID	21.38M	54.63	8.80M( $\times 2$ )	53.96	5.38M( $\times 3$ )	53.45	3.44M( $\times 4$ )	51.59	21.38M	<b>57.80</b>
		8.80M	54.54	5.38M	52.71	3.44M	51.27			<b>8.45M</b>	<b>57.77</b>
		5.38M	52.97	3.44M	50.60					<b>5.04M</b>	<b>57.82</b>
		3.44M	51.59							<b>3.33M</b>	<b>57.46</b>
	Non-IID	21.38M	52.88	8.80M( $\times 2$ )	<b>53.00</b>	5.38M( $\times 3$ )	52.23	3.44M( $\times 4$ )	50.19	21.38M	52.38
		8.80M	<b>52.57</b>	5.38M	51.59	3.44M	49.69			<b>8.45M</b>	52.37
		5.38M	51.55	3.44M	49.42					<b>5.04M</b>	<b>52.35</b>
		3.44M	49.35							<b>3.33M</b>	<b>51.75</b>
Fixed	IID	21.38M	49.54	8.80M( $\times 2$ )	50.15	5.38M( $\times 3$ )	50.79	3.44M( $\times 4$ )	51.59	21.38M	<b>57.72</b>
		8.80M	49.90	5.38M	48.08	3.44M	46.34			<b>8.45M</b>	<b>57.69</b>
		5.38M	48.98	3.44M	45.53					<b>5.04M</b>	<b>57.67</b>
		3.44M	46.52							<b>3.33M</b>	<b>57.49</b>
	Non-IID	21.38M	45.19	8.80M( $\times 2$ )	46.98	5.38M( $\times 3$ )	49.19	3.44M( $\times 4$ )	50.19	21.38M	<b>52.44</b>
		8.80M	46.14	5.38M	46.21	3.44M	44.33			<b>8.45M</b>	<b>52.48</b>
		5.38M	45.12	3.44M	42.68					<b>5.04M</b>	<b>52.48</b>
		3.44M	43.19							<b>3.33M</b>	<b>52.35</b>

Table 9. Top-1 test accuracy comparison with different methods on Tiny-ImageNet.

## C. Additional Experiments

### C.1. Performance under Homogeneous Setting

In Table 8, we evaluate different compression methods under homogeneous FL setting in terms of test Top-1 accuracy. It clearly shows that factorization compression outperforms the uniform pruning method in terms of accuracy, with a smaller model size. The computation overhead of low-rank model is higher than that of the width slimming model, as shown in Table 8. However, the bottleneck in FL is the communication cost [30]. Comparing with the original model, factorization compression can significantly reduce the communication cost by  $7.8\times$  to  $9.0\times$  and decrease the computation overhead by  $2.0\times$ . Note that on CIFAR-100, we directly compare the low-rank model (8.40M) with the original model (21.33M) and find that the

low-rank model outperforms the original model.

### C.2. Performance on Tiny-ImageNet

Table 9 shows the experiment results on Tiny-ImageNet under both dynamic and fixed heterogeneous settings. We can find in this table that FEDHM still shows superiority on the performance of small models. As shown in Table 8, under IID and Non-IID settings, training the smallest low-rank model (3.33M) homogeneously achieves 55.92% and 50.37% test accuracy on Tiny-ImageNet. When comparing them with the results in Table 9, we can also find that the smallest model gains 1.92% and 1.98% improvement under fixed heterogeneous setting. These results on the large datasets validate that FEDHM can significantly reduce the communication costs and improve the performance of the small models in various heterogeneous scenarios.